09

Influence of synthesis conditions on scintillation characteristics of ZnO tetrapods

© V.V. Krasnova [1], A.E. Muslimov [1], I.D. Venevtsev [2], M.P. Faradzheva [2], A.S. Lavrikov [1], L.A. Zadorozhnaya [1], V.M. Kanevsky [1]

[1] Shubnikov Institute of Crystallography of the Kurchatov Institute of Crystallography and Photonics, Moscow, Russia
[2] Peter the Great Saint-Petersburg Polytechnic University, St. Petersburg, Russia
E-mail: amuslimov@mail.ru

Received April 11, 2025
Revised June 16, 2025
Accepted June 17, 2025

The results of a comparative analysis of the morphology, structural and phase composition, and scintillation characteristics of ZnO tetrapods obtained by the carbothermal and gas-phase synthesis are presented. In the gas-phase synthesis, petal-type structures are formed along with classical tetrapods, crystalline quality increases, and scintillation characteristics of ZnO structures get improved. Due to the illumination time shortness, instantaneous intensity of the fast ultraviolet component with decay time of $\sim 0.7-1.0$ ns is two orders of magnitude higher than that of the slow component.

Keywords: zinc oxide, microscopy, luminescence, scintillators, tetrapods, petals.

DOI: 10.61011/TPL.2025.09.61819.20342

Zinc oxide (ZnO) is a unique material which, being exposed to ionizing radiation, exhibits luminescence kinetics of less than 1 ns [1–3]. Due to this, ZnO is regarded as the most promising scintillation material for studying rapidly changing processes. Ultrafast luminescence kinetics is inherent to only the ultraviolet luminescence (UVL) band associated with the exciton recombination in ZnO. On the contrary, the band of defect green luminescence (GL) is characteristic of ZnO structures with low crystalline quality and is accompanied by long-term luminescence kinetics. ZnO is distinct in a wide morphological diversity [4]: from uniaxial nano- and microcrystals to micropowders with hierarchical structure. Spectral position of the UV luminescence maximum in ZnO was found to depend on the sample synthesis conditions, structural perfection, and morphology [1,3,5–8]. The ZnO point-defect concentration correlates with the specific surface area [9] and, hence, increases with decreasing particle size. High concentration of defects may be assumed to induce a bandgap bend and red shift of the UV luminescence peak. However, the same study [9], as well as our experience in studying commercial nanoparticles, showed that the UV peak for ZnO nanoparticles is located, as in the case of bulk crystals, in the range of $373-383$ nm. Probably, the UV peak position in ZnO also depends on the predominant defectsńature. Despite this, the multiplicity of ZnO forms allows exploiting it in accordance with the tasks to be solved and with the scintillation element configuration.

Hierarchical structures of the ZnO microtetrapods (hereinafter tetrapods) consisting of wurtzite-structure single-crystal rods originating from the tetrahedron vertices [10] are distinguished by their high functionality. Previously [11,12] we have investigated ZnO tetrapods obtained by carbothermal synthesis involving doping the initial flux. The carbothermal synthesis specific feature is that in the crucible there is a narrow growth zone with supercritical oversaturation of zinc atoms. Above this zone, concentration of the zinc and oxygen atoms decreases sharply to minimum, and the tetrapod growth gets locked. As studies have shown, these conditions were ideal for synthesizing classical ZnO tetrapods. However, high growth rate made tetrapods to have large linear dimensions, low crystalline quality, and unsatisfactory scintillation characteristics. To slow down the growth process, it is necessary to expand the growth zone and reduce the gas-phase concentration of zinc atoms.

In this paper we propose transformation of the carbothermal synthesis into gas-phase one by removing carbon filters, and also comparative analysis of the structural-phase composition, luminescent properties and scintillation characteristics of ZnO tetrapods obtained by different methods.

The ZnO tetrapods were obtained by carbothermal synthesis according to the procedure described in [13]. As precursors, the following reagents were used: ACS-grade metallic Zn granules ~ 5 mm in diameter (99.999 %, metals basis, Alfa Aesar). In the carbothermal synthesis, ash-free cellulose filters served as a source of carbon. Tetrapods of two types were obtained: those involving carbon filters (type K) and free of carbon filters (type Γ). In both cases, the synthesis was performed in corundum crucibles at $1010\,^{\circ}$C with isothermal exposure for 50 min. Since the morphology and properties of ZnO tetrapods were strongly dependent on the sectoral position, samples for comparison were selected from the same sectors. Microscopic examination was performed using a Jeol Neoscope 2 (JCM-6000) scanning electron microscope (SEM). The X-ray phase analysis (XPA) was performed with diffractometer ARL X'TRA ThermoFisher (PANalytical, Netherlands) based on μ-radiation (1.5405 Å). To obtain a sufficient number of small, randomly oriented crystals, the powders were ground prior to studying. Photoluminescence (PL) spectra were

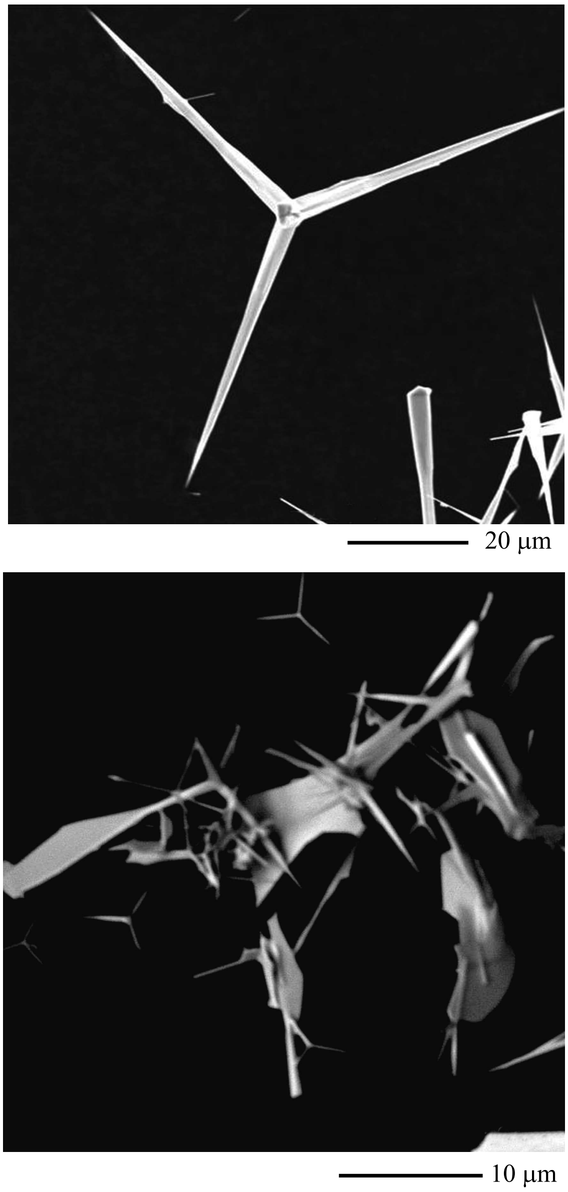

Figure 1. SEM images of the K-type microstructures (carbothermal synthesis) (*a*) and Γ-type microstructures (gas-phase synthesis) (*b*).

obtained on spectrofluorimeter CM 2203 (SOL-Instruments, Belarus). The X-ray luminescence (XRL) spectra were measured in the reflection geometry under continuous X-ray excitation (40 kV, 10 mA). At the given X-ray tube voltage, the main contribution comes from bremsstrahlung radiation with the maximum at $\sim 25-30$ keV. The sample radiation was detected with monochromator MDR-2 and photon counting system Hamamatsu H8259-01. The XRL kinetics was studied under pulsed X-ray excitation; the measurements were performed by the single-photon counting method using the setup described in [14].

According to XPA data, synthesized structures of the K- and Γ-types belong to the ZnO hexagonal wurtzite phase (JCPDS N 05-0664) [15]. The crystal lattice parameters are presented in the Table. As per the data obtained, carbothermal synthesis produces ZnO structures

Structural parameters of the synthesized samples

Type	$a = b$, Å	c, Å	V, Å^3
K	3.255	5.216	47.846
Γ	3.247	5.203	47.491
Standard [15]	3.247	5.203	47.491

with an increased lattice volume (an increase of about 1 %), while the gas-phase synthesis ensures parameters close to those of standard ZnO [15]. According to the electron microscopy data (Fig. 1), the K-type samples were classical tetrapods with the rod length of about $40-50\,\mu$m and core diameter amounting to $7-8\,\mu$m. In the case of gas-phase synthesis, large petal-type formations with lateral size of up to $8-10\,\mu$m and thickness of up to $5\,\mu$m were observed in addition to classical tetrapods with rod sizes of up to $10\,\mu$m. PL spectra (Fig. 2) for both sample types exhibit typical

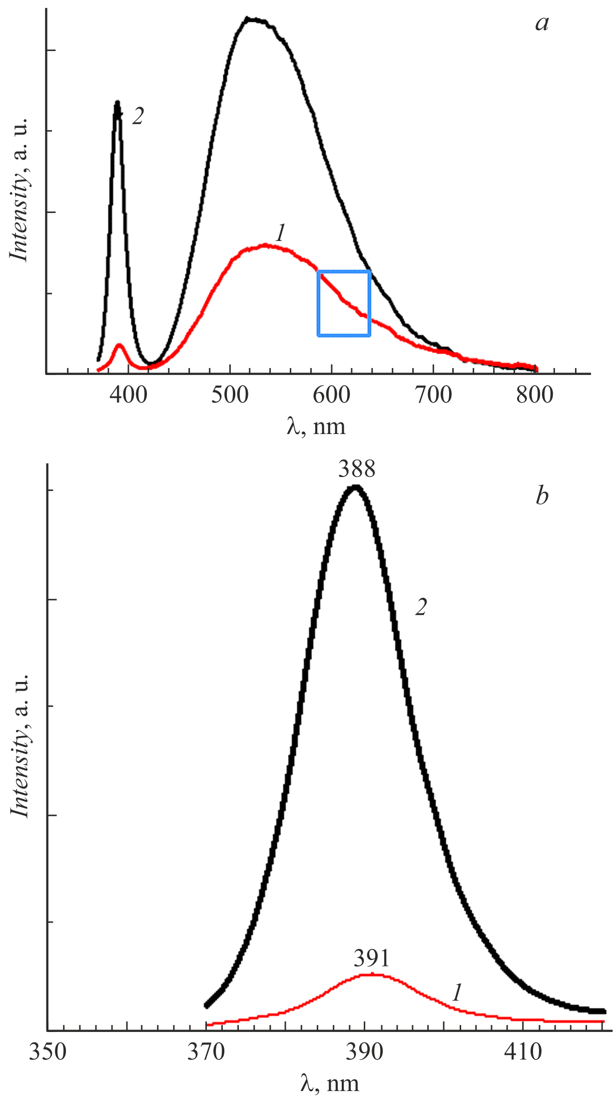

Figure 2. *a* — PL spectra of the K- and Γ-type microstructures; *b* — scaled-up UVL band of the samples' PL spectra. *1* — type K, *2* — type Γ. The frame shows the band of 590–630 nm corresponding to interstitial oxygen.

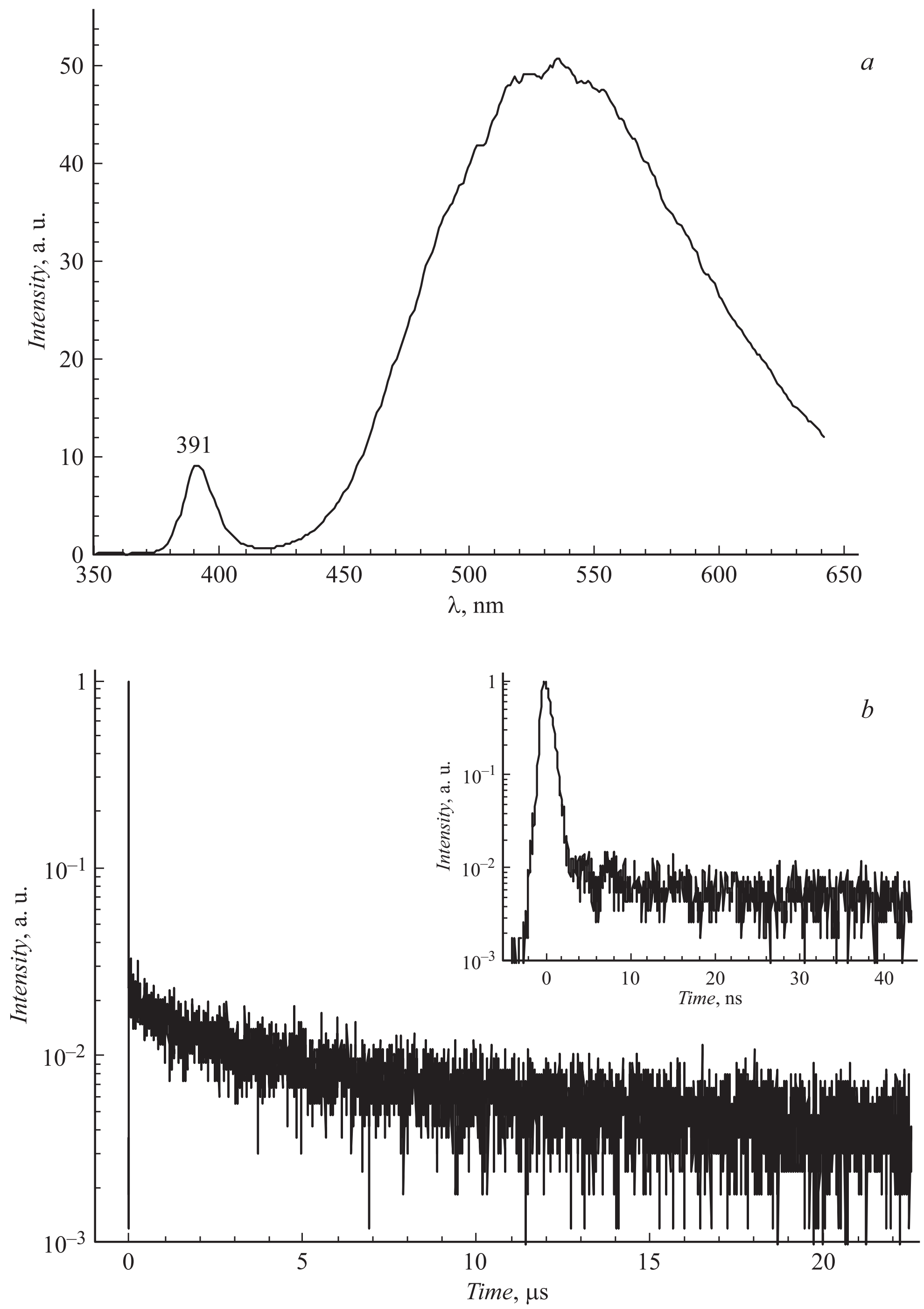

Figure 3. *a* — XRL spectrum of the Γ-type sample; *b* — luminescence kinetics of the Γ-type sample. The inset presents the kinetics part corresponding to fast UVL.

UVL and GL bands; however, the ratios between intensities I of their maxima are very different: ratios $I_{\mathrm{UVL}}/I_{\mathrm{GL}}$ for the K-type and Γ-type samples are 0.21 and 0.77, respectively. In addition, the 590–630 nm range of the K-type sample GL band (curve *1* in Fig. 2) exhibits an enhancement associated with interstitial oxygen [16].

Defects typical of ZnO are oxygen vacancies, which makes ZnO an *n*-type semiconductor. The presence of interstitial oxygen O_i^{2-} is generally considered low-probable because of its large ionic radius (140 pm). However, the XPA and PL results for the K-type sample confirm a high content of interstitial oxygen, which induces expansion of the crystal lattice. At the stage of the ZnO tetrapods nucleation, a sphalerite core gets formed [17]. Then four wurtzite rods begin growing from the core. It is possible to assume that, when zinc concentration is high and growth zone is narrow, the rods grow not only from adatoms but also from the Zn–O system clusters forming in the gas phase. In this case, formation of the structure proceeds with capturing atoms that diffuse in the gas phase and have no time to integrate into the ZnO matrix. This model may explain the ZnO tetrapods' high growth rate, concentration and, hence, defectiveness in the carbothermal synthesis. It is important to note that interstitial oxygen deforms the lattice throughout the entire bulk. Therefore, an intense broad-band GL is observed in both the PL and XRL spectra in the case of excitation by deeply penetrating X-ray radiation. During the gas-phase synthesis, zinc concentration in the growth zone decreases due to the zone broadening. Therewith, the rate of spontaneous tetrapod nucleation in the gas phase decreases but, at the same time, conditions for secondary nucleation arise on the faces and edges of the formed tetrapods. This is what explains formation of the petal-type structures. In addition, in the carbothermal synthesis there may be observed a red shift of the UVL peak (Fig. 2, *b*) and deterioration of the tetrapod crystalline quality.

The XRL spectrum of the Γ-type tetrapods shown in Fig. 3, *a* contains both the UVL band of 370−420 nm and GL band of 460−650 nm. The UVL maximum is located at the wavelength of 391 nm. Intensity of this band is about 2.5 % of the integral intensity. The XRL kinetics is shown in Fig. 3, *b* in two ranges: from 0 to 20 μs and from 0 to 40 ns (in the inset), where 0 is the time moment corresponding to the maximum radiation intensity. The decay time was approximately estimated through monoexponential approximation in relevant time intervals. Intense radiation in the nanosecond range corresponds to UVL. If the exciting pulse width (about 0.8 ns) is not taken into account, the decay time of this radiation is 0.7−1.0 ns, and its intensity is about 5 % of the total intensity. The difference of this proportion from that obtained by spectral measurements is caused by the difference in irradiation conditions. The figure shows that luminescence within the range under consideration decays incompletely, which may cause underestimation of the total intensity. The slow green luminescence decays non-exponentially. The characteristic time may be approximately estimated as 4−6 μs. Despite the UVL fraction is small, shortness of its luminescence lifetime makes its instantaneous intensity two orders of magnitude higher than that of GL.

The paper presents the results of comparative analysis of the structural-phase composition and spectral-kinetic properties of ZnO samples obtained by the carbothermal and gas-phase synthesis. The study has shown that the gas-phase synthesis produces, along with classical tetrapods, structures of the petal type. Therewith, the crystalline quality improves, and ultraviolet luminescence band gets enhanced. In addition, the study has revealed a red shift of the UVL peak along with deterioration of the tetrapods' crystalline quality. Fast X-ray excited luminescence has a maximum at 391 nm; its intensity is 2.5−5 % of the integral intensity. At the same time, the intensity of pulse-excited UVL is approximately two orders of magnitude higher than that of GL.

Funding

The study was supported by the Russian Science Foundation, project No 24-29-00696, https://rscf.ru/project/24-29-00696/).

Conflict of interests

The authors declare that they have no conflict of interests.

References

[1] Y. Furukawa, M. Tanaka, T. Nakazato, T. Tatsumi, M. Nishikino, H. Yamatani, T. Fukuda, J. Opt. Soc. Am. B, **25** (7), B118 (2008). DOI: 10.1364/josab.25.00b118

[2] M. Cadatal-Raduban, J. Olejnicek, K. Hibino, Y. Maruyama, A. Pisarikova, K. Shinohara, T. Asaka, L.L. Volfova, M. Kohout, Z. Jiaqi, Y. Akabe, M. Nakajima, J.A. Harrison, R. Hippler, N. Sarukura, S. Ono, Z. Hubicka, K. Yamanoi, Adv. Opt. Mater., **12** (21), 2400377 (2024). DOI: 10.1002/adom.202400377

[3] I.D. Venevtsev, A.P. Tarasov, A.E. Muslimov, E.I. Gorokhova, L.A. Zadorozhnaya, P.A. Rodnyi, V.M. Kanevsky, Materials, **14** (8), 2001 (2021). DOI: 10.3390/ma14082001

[4] D.K. Sharma, S. Shukla, K.K. Sharma, V. Kumar, Mater. Today: Proc., **49**, 3028 (2020). DOI: 10.1016/j.matpr.2020.10.238

[5] P.T. Hsieh, Y.C. Chen, K.S. Kao, M.S. Lee, C.C. Cheng, J. Eur. Ceram. Soc., **27** (13-15), 3815 (2007). DOI: 10.1016/j.jeurceramsoc.2007.02.053

[6] J. Ji, A.M. Colosimo, W. Anwand, L.A. Boatner, A. Wagner, P.S. Stepanov, T.T. Trinh, M.O. Liedke, R. Krause-Rehberg, T.E. Cowan, F.A. Selim, Sci. Rep., **6**, 31238 (2016). DOI: 10.1038/srep31238

[7] M.J.F. Empizo, K. Fukuda, R. Arita, Y. Minami, K. Yamanoi, T. Shimizu, R.V. Sarmago, Opt. Mater., **38**, 256 (2014). DOI: 10.1016/j.optmat.2014.10.044

[8] L. Kumar, Y. Kumari, A. Kumar, M. Kumar, K. Awasthi, Mater. Chem. Front., **1** (7), 1413 (2017). DOI: 10.1039/c7qm00058h

[9] X. Zhang, J. Qin, Y. Xue, P. Yu, B. Zhang, L. Wang, R. Liu, Sci. Rep., **4** (1), 4596 (2014). DOI: 10.1038/srep04596

[10] O.A. Lyapina, A.N. Baranov, G.N. Panin, A.V. Knotko, O.V. Kononenko, Inorg. Mater., **44** (8), 846 (2008). DOI: 10.1134/S0020168508080116.

[11] I.D. Venevtsev, A.E. Muslimov, L.A. Zadorozhnaya, A.S. Lavrikov, P.A. Rodnyi, V.M. Kanevskii, Opt. Spectrosc., **128** (11), 1784 (2020). DOI: 10.1134/S0030400X20110272.

[12] A.E. Muslimov, A.D. Tsarenko, A.S. Lavrikov, A.A. Ulyankina, V.M. Kanevskii, Tech. Phys. Lett., **49** (8), 45 (2023). DOI: 10.61011/TPL.2023.08.56687.19577.

[13] [L.N. Demyanets, L.E. Li, A.S. Lavrikov, S.V. Nikitin, Crystallogr. Rep., **55** (1), 142 (2010). DOI: 10.1134/S1063774510010219.

[14] P.A. Rodnyi, S.B. Mikhrin, A.N. Mishin, A.V. Sidorenko, IEEE Trans. Nucl. Sci., **48** (6), 2340 (2001). DOI: 10.1109/23.983264

[15] *Joint Committee on Powder Diffraction Standards* (*JCPDS*), file N 05-0664.

[16] K. Kocsis, M. Niedermaier, J. Bernardi, T. Berger, O. Diwald, Surf. Sci., **652**, 253 (2016). DOI: 10.1016/j.susc.2016.02.019

[17] Y. Ding, Z.L. Wang, T. Sun, J. Qiu, Appl. Phys. Lett., **90**, 153510 (2007). DOI: 10.1063/1.2722671

Translated by EgoTranslating